

# Dynamic Tests and Simulation of Magneto-Rheological Dampers

Hiroshi Sodeyama\*, Katsuaki Sunakoda

*Sanwa Tekki Corporation, 2703, Naka-okamoto, Kawachi-machi, Tochigi, 329-1192, Japan*

Hideo Fujitani

*Building Research Institute, Tatehara 1, Tsukuba-shi, Ibaraki, 305-0802, Japan*

Satsuya Soda

*Waseda University, 3-4-1, Okubo, Shinjuku-ku, Tokyo, 169-8555, Japan*

Norio Iwata

*Kinki University, 3-4-1, Kowakae, Higashi-osaka-shi, Osaka, 577-8502, Japan*

&

Katsuhiko Hata

*Bando Chemical Industries, Ltd., 3-1-6, Ashihara-dori, Hyogo-ku, Kobe, 652-0882, Japan*

**Abstract:** *Magneto-rheological fluid dampers (MR dampers) have recently been designed to control the response of civil engineering and building structures because of their large force capacity and controllable force characteristics. To enable them to control structural responses, the dynamic characteristics of structures need to be clarified. This paper discusses the design of MR dampers with a bypass orifice mechanism and verifies their performance by means of dynamic tests and dynamic analytical models. Their dynamic characteristics are investigated experimentally to compare the performance of two different magneto-rheological fluids. One is developed by the Lord Corporation and the other is newly developed in Japan. The effectiveness and validity*

*of MR dampers with a bypass are discussed on the basis of these results.*

## 1 INTRODUCTION

In recent years, many active vibration control systems have been adopted in civil engineering and building structures. Active vibration control systems such as active mass dampers have shown excellent vibration mitigation effects compared with the passive vibration control systems. However, there are some problems with respect to reliability and cost performance. Semi-active vibration control has also attracted a great deal of attention. Semi-active vibration control systems are different from active vibration control systems, which directly suppress vibrations by means of a large amount of externally

\*To whom correspondence should be addressed. E-mail: [sodeyama@tekki.co.jp](mailto:sodeyama@tekki.co.jp).

supplied energy. Semi-active vibration devices alter their damping characteristics according to an external command. Therefore, a comparatively high vibration mitigation effect can be obtained by means of semi-active vibration control without major power consumption.

One conventional semi-active vibration device was developed using viscous dampers. Adjusting the opening rate of the flow control valves inside the viscous damper changes their damping characteristics. Semi-active viscous dampers are already being utilized in some engineering fields, and their vibration mitigation effects are proved by Niwa et al. (1998) and Kurita et al. (1998).

Magneto-rheological fluid dampers (MR dampers) have been developed as semi-active vibration devices in recent years by Carlson and Spencer (1996), Spencer et al. (1997, 1998), Johnson et al. (1998), and Jolly et al. (1999). As their operating fluid, they use a magneto-rheological fluid that responds to applied magnetic fields. Magneto-rheological fluids alter their viscosity according to the applied magnetic field and exhibit nonlinear properties like a typical Bingham fluid. In MR dampers, electromagnets are used to generate the required magnetic field. The force generated in the MR damper is therefore controllable by adjusting the electric current supplied to the electromagnets. The response time of commercial magneto-rheological fluids is extremely rapid, being in the order of milliseconds. MR dampers thus achieve rapid response to command signals because they have no mechanical mechanism for generating the controllable force.

MR dampers have been studied by Spencer and Carlson. The Lord Corporation has already developed commercial MR dampers with an approximate maximum force of 3 kN, and Spencer and Carlson have developed a large-scale, 200 kN MR damper for seismic response mitigation of real building structures. Semi-active control of building structures using controllable fluid dampers is being studied in the U.S.–Japan cooperative research and development project of Smart Materials and Structural System launched in 1998 by the U.S. National Science Foundation and the Building Research Institute, Japan Ministry of Construction. This paper deals with one of the results achieved by the ER/MR working group in the Effector section on the Japanese side of this cooperative project. The object of this study is to develop an MR damper that enables effective semi-active control of real building structures and several civil engineering structures. 2 kN, 20 kN, and 200 kN MR dampers have been developed in this study as prototypes. A new mechanism, a bypass type magnetizing orifice mechanism, has been adopted in order to expand design flexibility for electromagnets. A new magneto-rheological fluid has also been evaluated. Two types of magneto-rheological fluids have been tested.

One is a typical commercial magneto-rheological fluid, MRF-132LD, produced by the Lord Corporation, and the other is a new trial product #104 made on an experimental basis by Bando Chemical Industries in Japan.

## 2 STRUCTURE OF BYPASS TYPE MR DAMPERS

Figure 1 shows the hydraulic circuit of the most primitive bypass type MR damper. This hydraulic system has been adopted for the 2 kN MR and 20kN MR dampers developed in this study as prototypes. The damper has a symmetric structure because it utilizes a double-ended piston. The cylinder is divided into two airtight pressure chambers by a piston with rubber O-rings. Therefore, the bypass flow portion installed under the cylinder is only a passage connecting two pressure chambers. However, another similar flow passage for the magneto-rheological fluid exists above the cylinder. Two check valves are set up in this flow passage, and the fluid flow from the pressure chambers is stopped while the MR damper is operating. This flow passage, including the reservoir, is used to compensate for fluid expansion due to temperature increase of the magneto-rheological fluid. The bypass flow portion has an orifice with a short length for magnetizing the magneto-rheological fluid. An electromagnet is installed in this orifice and is used to generate the variable magnetic field. As shown in Figure 1, the electromagnet is composed of a steel yoke and a coil. The yoke is of low carbon steel to ensure high magnetic performance, that is, a high level of magnetic saturation and low residual magnetization. The yoke is C shaped, and the orifice is located in the space between the ends of the yoke. Copper wire is wound around the steel yoke. This magnetizing system has several advantages. Because the electromagnet is not in direct contact with the magneto-rheological fluid, there is an extremely small temperature increase in the fluid due to the heat generated in the coil. Magneto-rheological fluid viscosity generally decreases with temperature, which also decreases the damping force. Thus, the ability to suppress the influence of heat generated in the coil is one of the most important factors in the design of MR dampers. A rectangular orifice cross-section is selected to generate a uniform magnetic field at the orifice. An intense magnetic flux is applied to the magneto-rheological fluid perpendicular to the orifice. This magnetic field generates a yield stress in the magneto-rheological fluid.

Figures 2 and 3 show photographs of a 2 kN MR damper and a 20 kN MR damper, respectively. Table 1 shows their design specifications. The two dampers have almost identical electromagnets, the specifications of which are shown in Table 1. Two of the most important specifications, the number of turns on the coil and the size

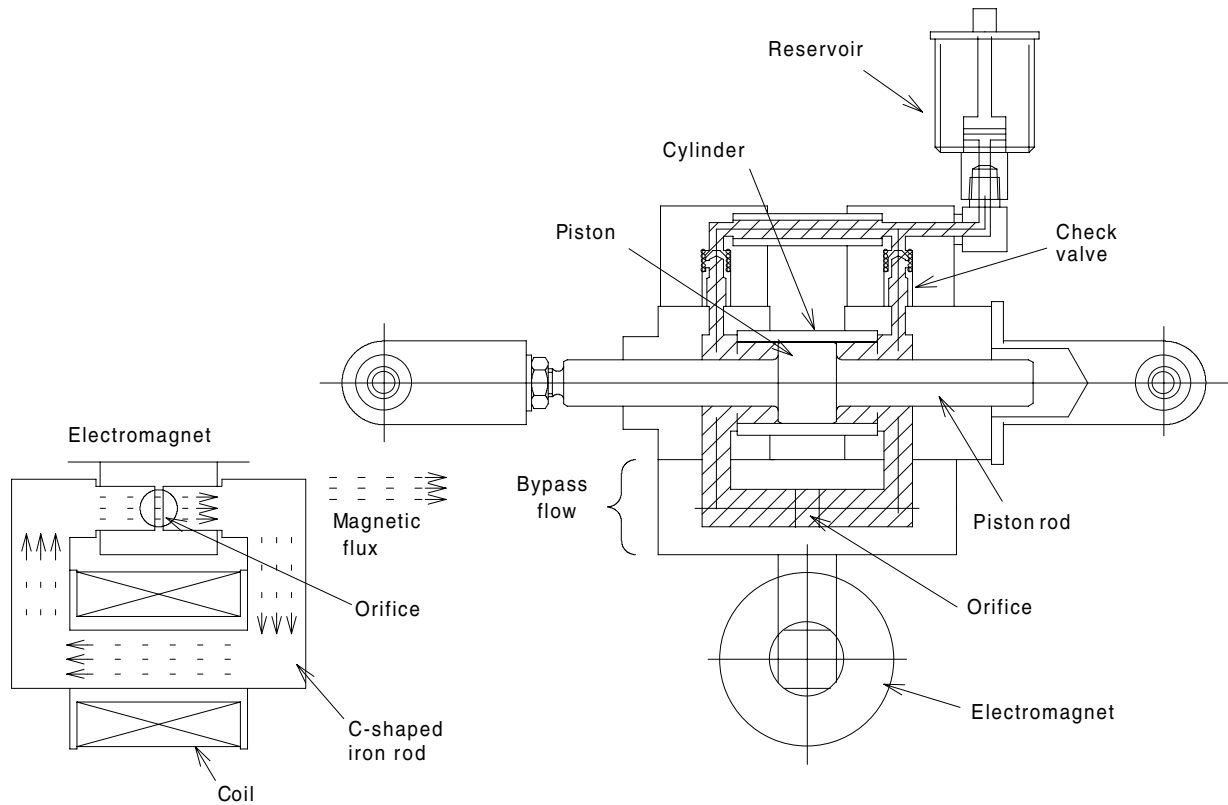


**Fig. 1.** Hydraulic circuit of bypass-type MR damper.

of the steel yoke, are exactly the same. The only differences are the orifice gap and the orifice length. In order to suppress the rise of viscous force and to increase the space in which the magnetic flux penetrates the magneto-rheological fluid flow, the 20 kN MR damper's orifice is longer and wider. Therefore, the 20 kN MR damper needs twice the applied current to the electromagnet in order to generate the required magnetic field. How-

ever, the maximum required electric power is only about 10 W.

Figure 4 shows a cross-sectional view of the 200 kN MR damper for vibration control of full-scale civil engineering structures. Figure 5 shows a photograph of the 200 kN MR damper developed in this study. The basic mechanism is similar to the previous 2 kN and 20 kN MR dampers. This 200 kN MR damper also has a bypass

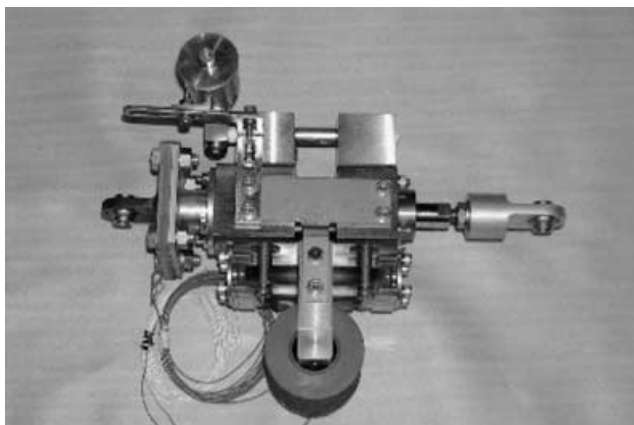


**Fig. 2.** 2 kN MR damper.



**Fig. 3.** 20 kN MR damper.

**Table 1**  
Design specifications of MR dampers

	<i>MR damper</i> –2 kN	<i>MR damper</i> –20 kN
Max. force (nominal)	2 kN	20 kN
Stroke	±10 mm	±35 mm
Cylinder bore	35 mm	95 mm
Orifice size	0.6 × 16 mm	2 × 20 mm
Orifice length	10 mm	20 mm
MR fluid	MRF-132LD	MRF-132LD
Coil	φ0.5 mm	3800 turns
Inductance		1.5 henries
Coil resistance		60 ohms
Max. current	0.08 A	0.16 A

portion with an electromagnet. The annular spaces between the outer cylinder and inner coils (magnetic poles) form the orifices. The orifice portions are divided into ten stages by the coils. Each coil is electrically connected in series and is applied a constant electrical current. The marching coils are wound in opposite directions, so it is possible to obtain effective magnetic circuits between the magnetic poles, as shown in Figure 6. The magnetic flux is basically applied perpendicularly to the magneto-rheological fluid flow at every stage. Dwarfing of the electromagnet to decrease power consumption is achieved by installing the electromagnet at the bypass portion and dividing the magnetizing spaces into several small subspaces.

Table 2 shows the design specifications of the 200 kN MR damper. Trial product #104 made by Bando Chemi-

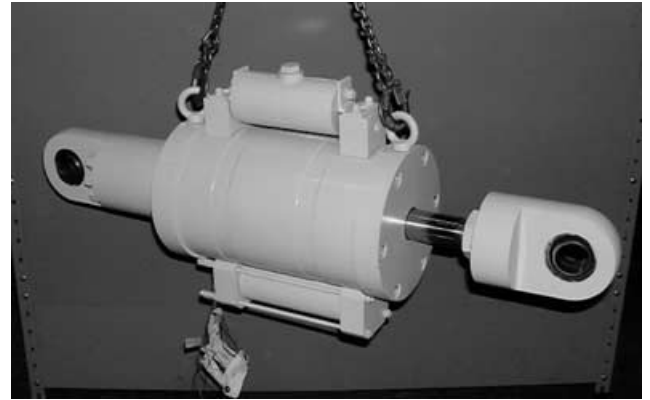


**Fig. 5.** 200 kN MR damper.

cal Industries is tested and evaluated using this MR damper and a new developed magneto-rheological fluid. This fluid is a silicone-based magneto-rheological fluid containing a similar proportion of micron-sized ferromagnetic particles to the conventional commercial magneto-rheological fluid, Lord MRF-132LD.

### 3 EXPERIMENTAL INVESTIGATION OF DYNAMIC CHARACTERISTICS

Various dynamic tests have been carried out on the developed MR dampers using the vibration testing facilities at Sanwa Tekki Corporation and at the Building Research Institute. The actuator of the vibration testing facility at STC has a maximum velocity of 40 cm/s and a maximum displacement of 40 mm. The one at BRI has

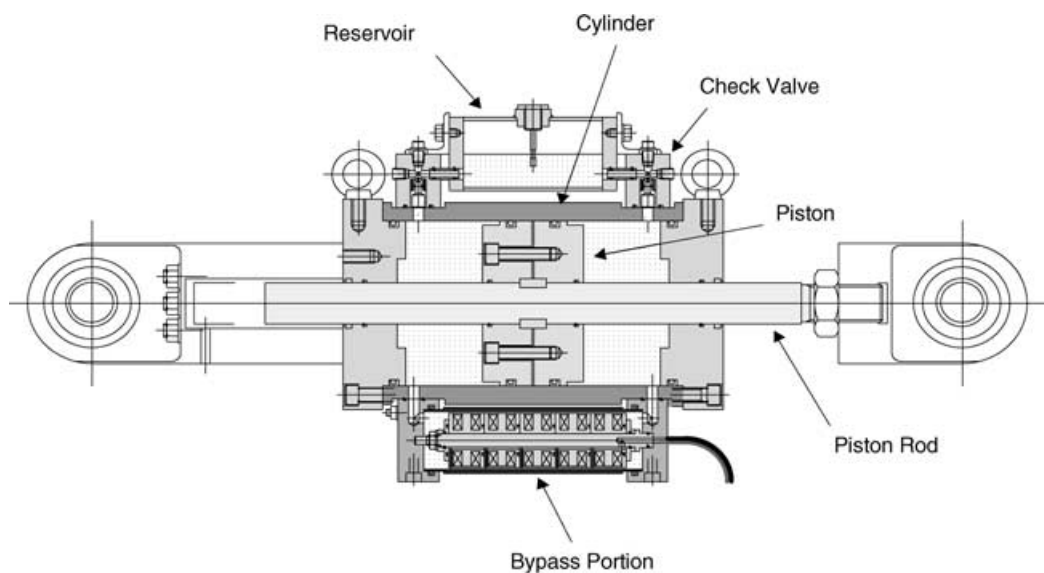


**Fig. 4.** Cross-sectional view of 200 kN MR damper.

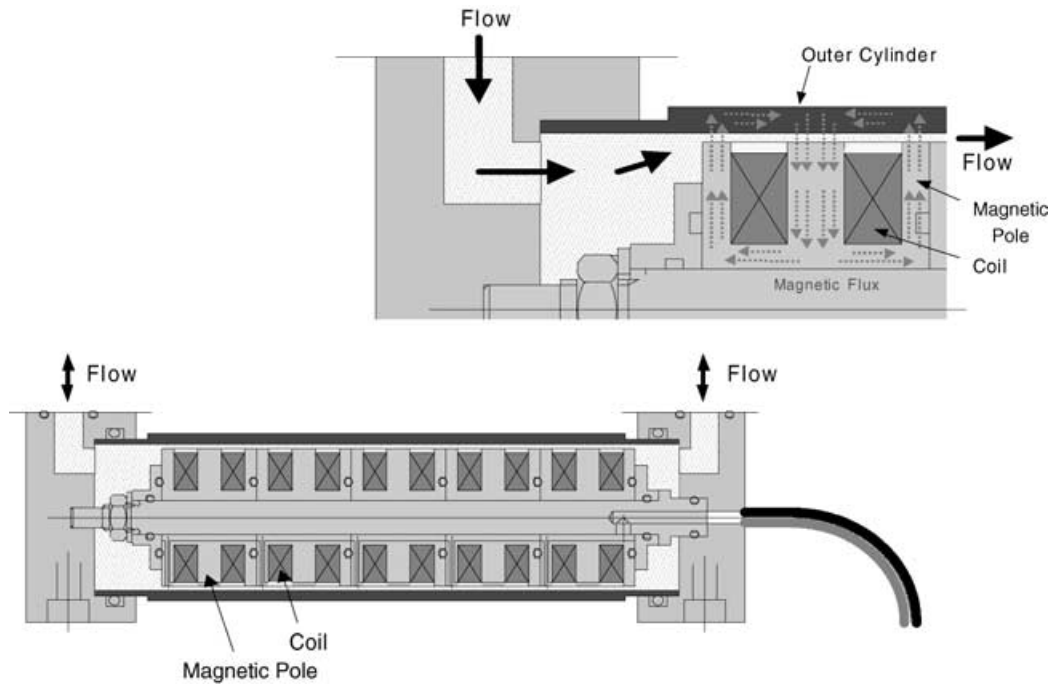


**Fig. 6.** Cross-sectional view of bypass portion of 200 kN MR damper.

a maximum displacement of 200 mm and a maximum velocity of 20 cm/s. The dynamic tests on the 200 kN MR damper were conducted using both testing facilities to utilize the merits of each. Figure 7 shows a schematic diagram of the experimental setup for the dynamic tests. A sinusoidal or triangular input displacement was applied to the MR dampers and the generated forces were measured by the load cell. The force–displacement loops and force–velocity relationships were evaluated. The in-

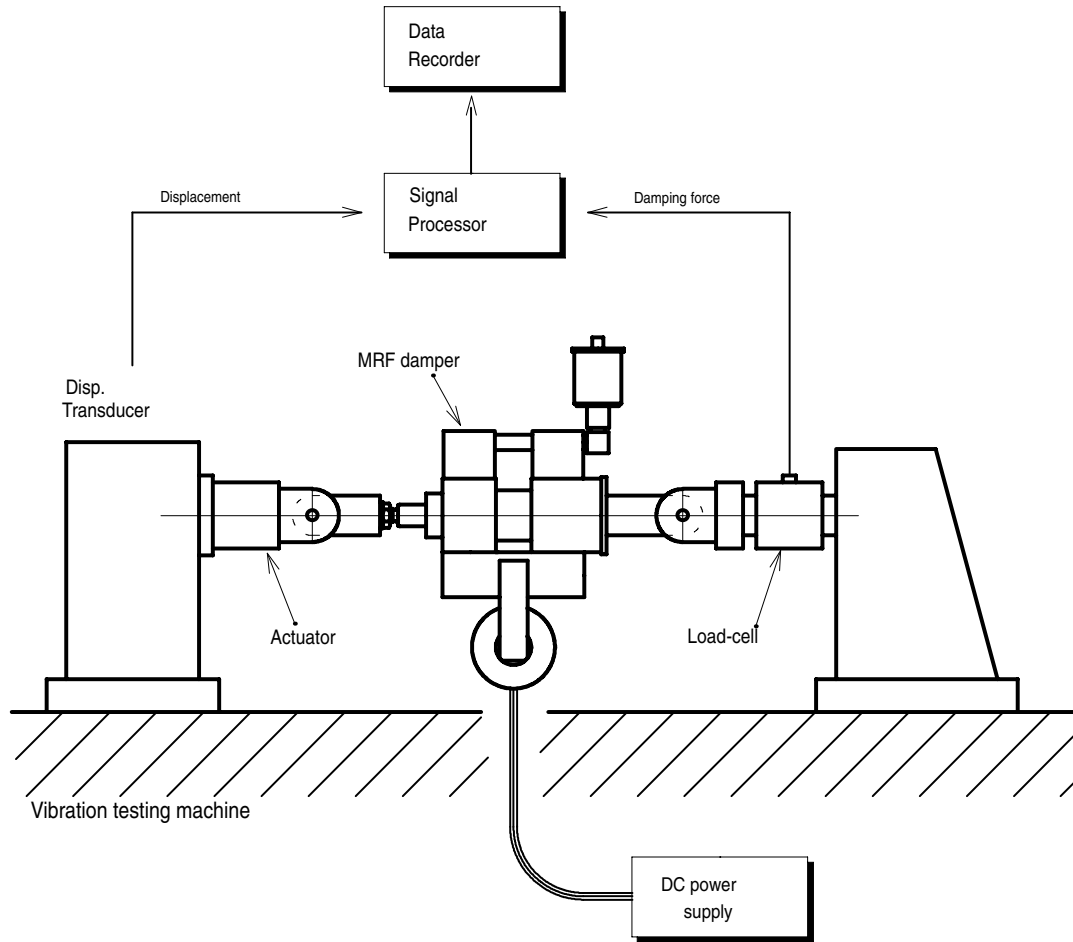
put current to the electromagnet was also a significant test parameter.

Figure 8 shows the test results for the 2 kN MR damper. The figure shows the force–displacement loops under the sinusoidal waveform movement with maximum input velocities of 5 cm/s, 9 cm/s, and 20 cm/s. The dynamic tests on the 2 kN MR damper were conducted under input electric currents of 0 A, 0.016 A, 0.032 A, 0.048 A, 0.064 A, and 0.08 A. It was verified that maximum damping force was controllable by adjusting the strength of the applied magnetic field. Furthermore, an upper limit of the controllable force was observed. Figure 9 shows the relationship between the maximum velocity of the piston and the maximum force generated in the 2 kN MR damper.

The force–displacement loops shown in Figure 10 are the experimental results for the 20 kN MR damper. These tests were conducted under the sinusoidal waveform input with a frequency of 0.25 Hz and a magnitude of 20 mm (zero to peak). In these tests, the only difference was the current applied to the electromagnet. Figure 11 shows the relationship between the input current and the maximum generated force. It is confirmed that the maximum damping force also rises with the increase in the applied current in the same way as the previous 2 kN MR damper. An upper limit is also observed in Figure 11. Figure 12 shows the measured magnetic flux at the orifice portion of 20 kN MR damper. The magnetic

**Table 2**  
Design specifications of 200 kN MR damper

<i>MR damper (200 kN)</i>	
Max. force (Nominal)	200 kN
Stroke	±80 mm
Cylinder bore	200 mm
Bypass portion (Annular orifice)	Outer diameter: 70 mm Inner diameter: 66 mm Length of magnetic field: 10 mm × 10 stages
MR fluid	a. LORD Corp.: MRF-132LD b. Trial product #104
Electromagnet	Coil 0.8 mm, 2200 turns Inductance 0.11 henries Resistance 10.5 ohms
Max. current	5 A



**Fig. 7.** Experimental setup for dynamic test of MR damper.

flux at the orifice with the magneto-rheological fluid saturates in a similar manner to the generated force of the MR damper over an applied current of approximately 0.2 A. It is thus understood that the upper limit of the controllable force is fixed by the magnetic property of

the magneto-rheological fluid, that is, the level of magnetic saturation. Figures 13 and 14 show the other experimental results for the 20 kN MR damper. These test results are measured for several sinusoidal waveform inputs. The force–displacement loops under no magnetic

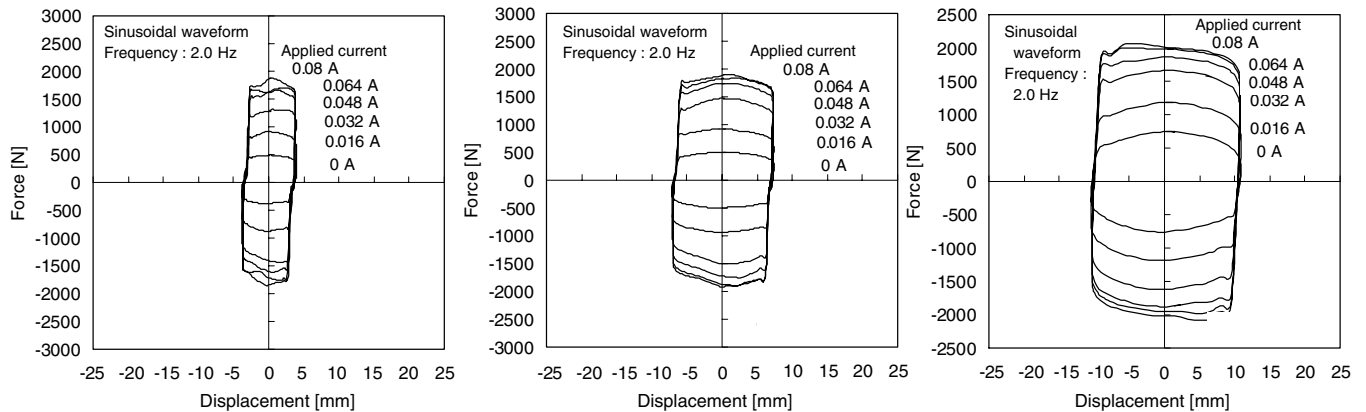


**Fig. 8.** Force–displacement loops of 2 kN MR damper.

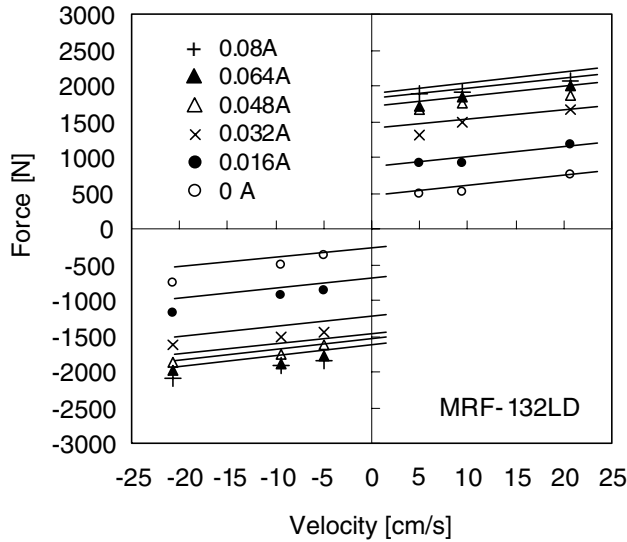


Fig. 9. Force–velocity relationship of 2 kN MR damper.

field exhibit the behavior of a typical viscous damper. For the 2 kN MR damper, the friction force of the sealing or the damping force due to the residual magnetization is dominant for the total generated force, because the magnitude of the generated force is comparatively small. Therefore, the shape of the loops with no field is close to the friction type of damping characteristic. For the 20 kN MR damper, these initial forces are negligible. Through these dynamic tests, it is experimentally confirmed that a controllable force can be obtained at very low speeds and a very small displacement range.

Figure 15 shows the force–displacement loops of the 200 kN MR damper under the sinusoidal loading. The performances of this damper using two different magneto-rheological fluids were investigated and compared. One fluid was MRF-132LD, used in other

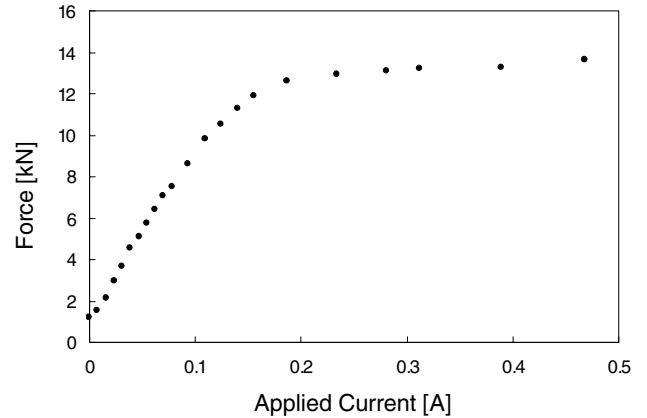


Fig. 11. Applied current–force relationship of 20 kN MR damper.

MR dampers developed in this study. The other was the newly developed magneto-rheological fluid, trial product #104 made by Bando Chemical Industries. Both fluids have almost the same percentage of micron-sized ferromagnetism particles. However, they use quite different base oils. Trial product #104 is a silicone based magneto-rheological fluid and has a higher viscosity than MRF-132LD. Therefore, the MR damper filled with trial product #104 generated larger forces. For the 200 kN MR damper, the force–displacement loops measured in the high-speed range show a specific tendency to lean to the left, suggesting a negative stiffness. This seems to be caused by the inertia force of the piston mass and the fluid mass. Figure 16 shows the force–velocity relationship of the 200 kN MR damper. It was also verified experimentally that the controllable range established by trial product #104 was wider than that of MRF-132LD. The controllable range is defined as the difference between

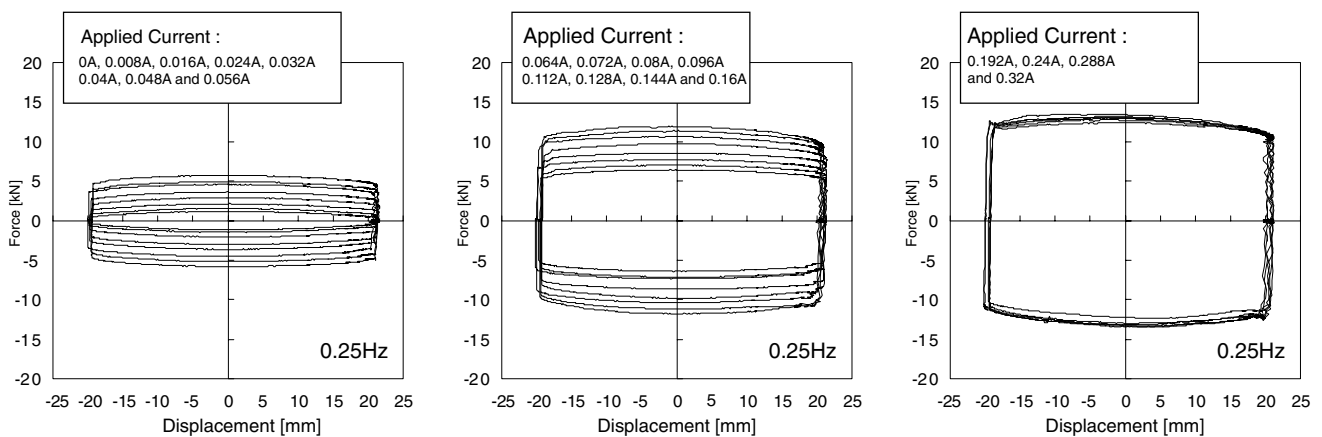
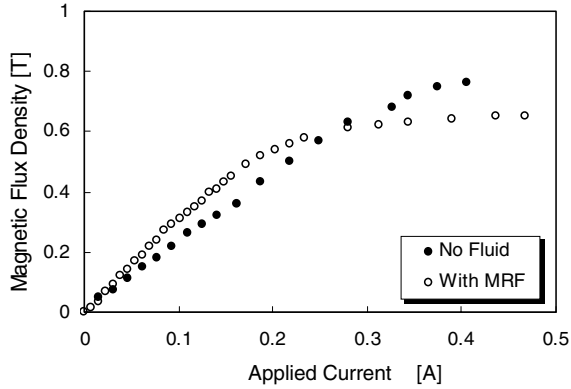


Fig. 10. Force–displacement loops of 20 kN MR damper; sinusoidal input 0.25 Hz,  $\pm 20$  mm.



**Fig. 12.** Applied current–magnetic flux density relationship of 20 kN MR damper.

the generated force without the magnetic field and the generated force with the magnetic field.

#### 4 ANALYTICAL MODELS FOR PREDICTING PERFORMANCE

This section proposes analytical models for simulating the dynamic behavior of the MR dampers, and it compares the simulation results with the experimental results. Many types of analytical models have been pro-

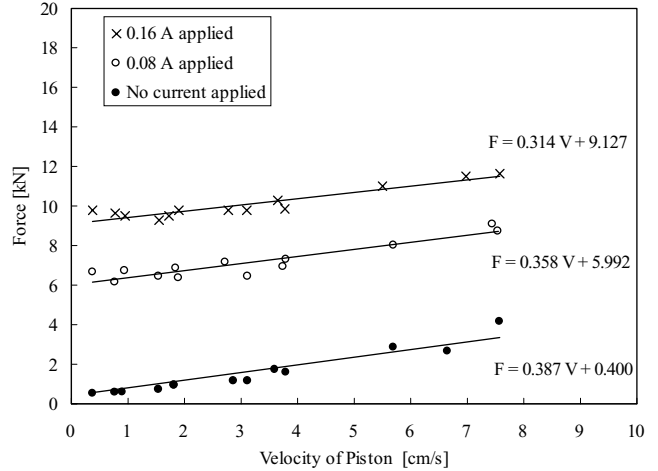


**Fig. 14.** Force–velocity relationship of 20 kN MR damper.

posed for MR or ER dampers. Gavin used the mechanical model proposed by Gamota to simulate the dynamic behavior of ER dampers, in which the Zener element shows frequency dependent behavior over a wide range of frequencies. Spencer et al. (1997, 1998) proposed a simulation model consisting of two springs, two dashpots, and the Bouc-Wen model. This model can also exactly predict the dynamic behavior of both the

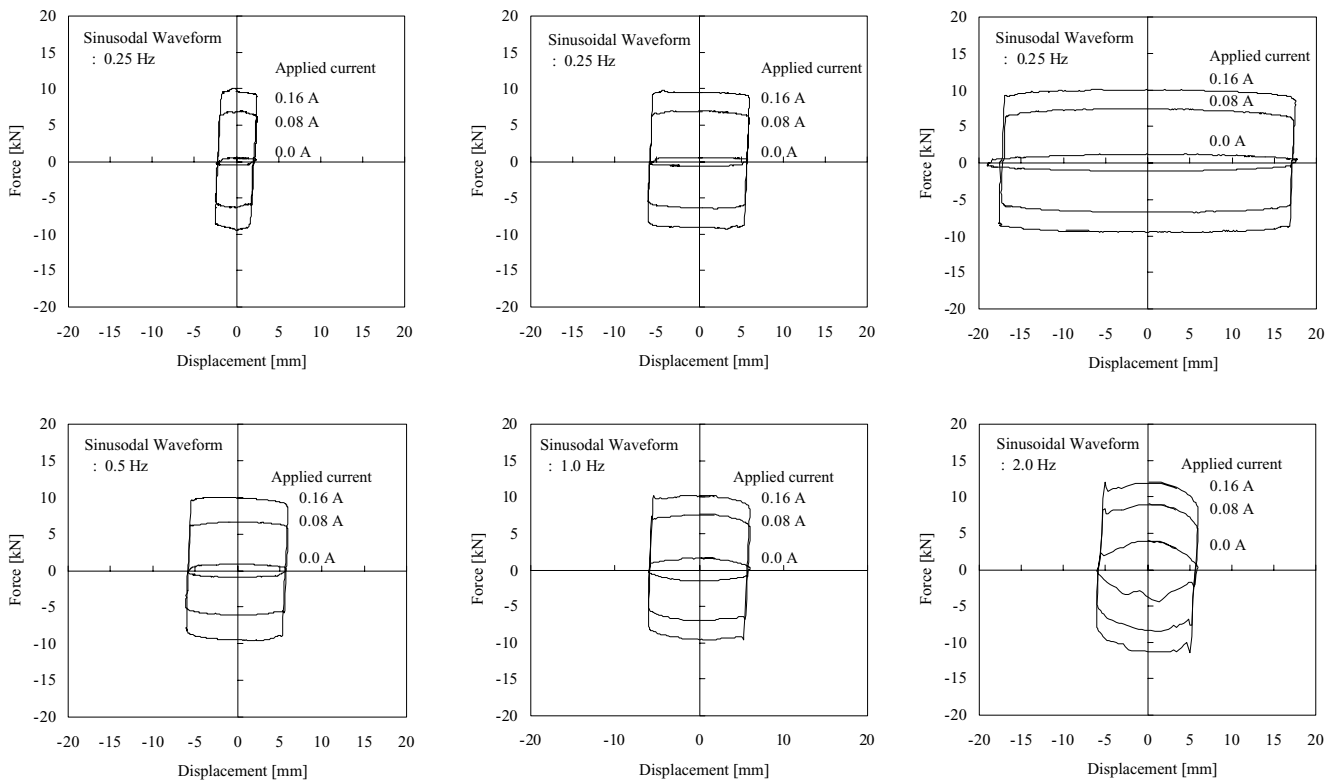


**Fig. 13.** Force–displacement loops of 20 kN MR damper.

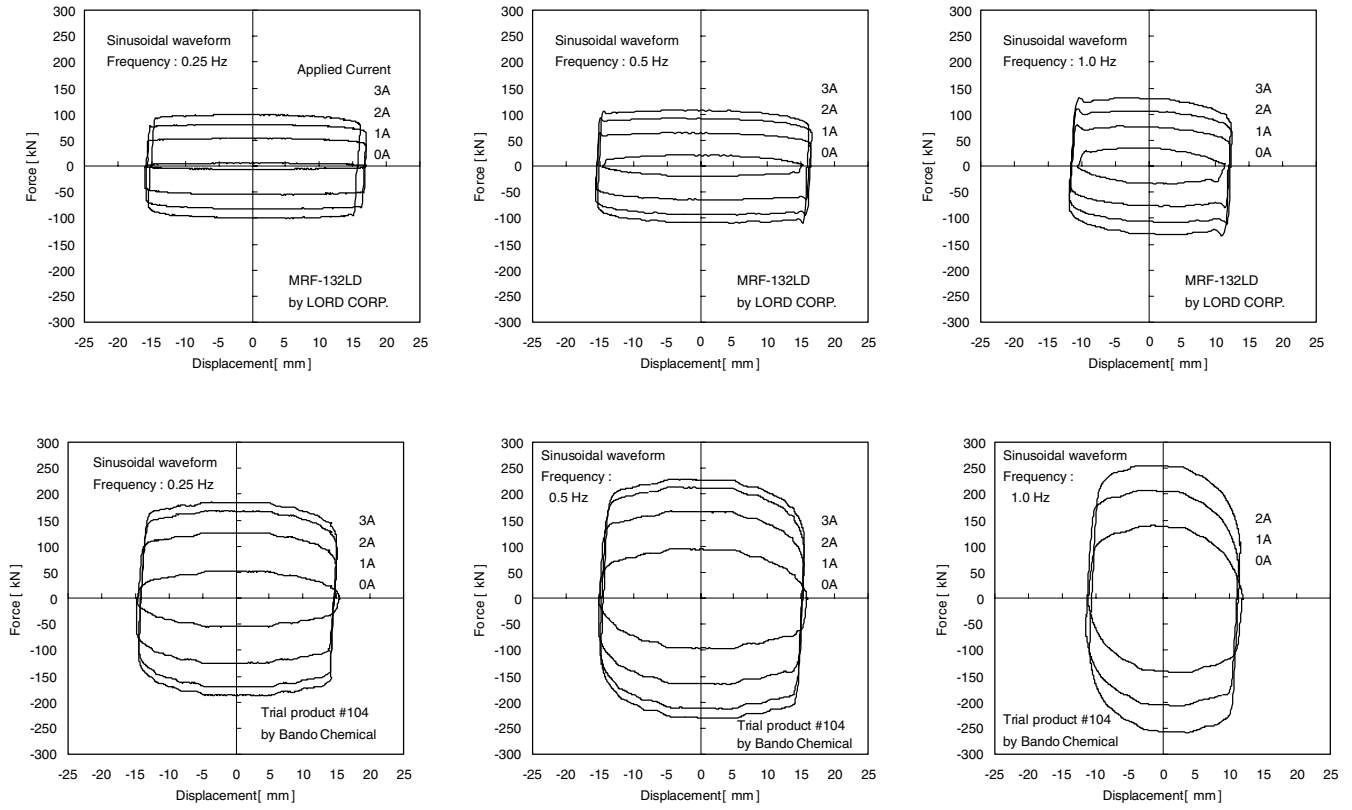


Fig. 15. Force–displacement loops of 200 kN MR damper.

force–displacement characteristic and the force–velocity relationship for MR dampers. In contrast to those complicated multi-element models, the authors aim at simulating the behavior of MR dampers with simple analytical models. Two models are considered. One is a

Bingham model, in which a couple comprising a dash-pot and a friction slider are connected in parallel. This Bingham model has been used to simulate the behavior of MR dampers in some studies, and it is verified that it can predict the force–displacement relationship well

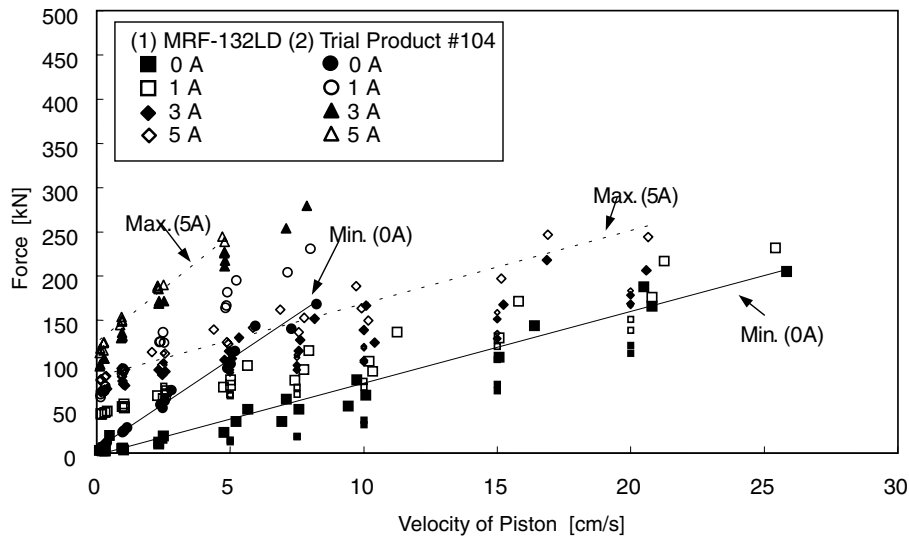
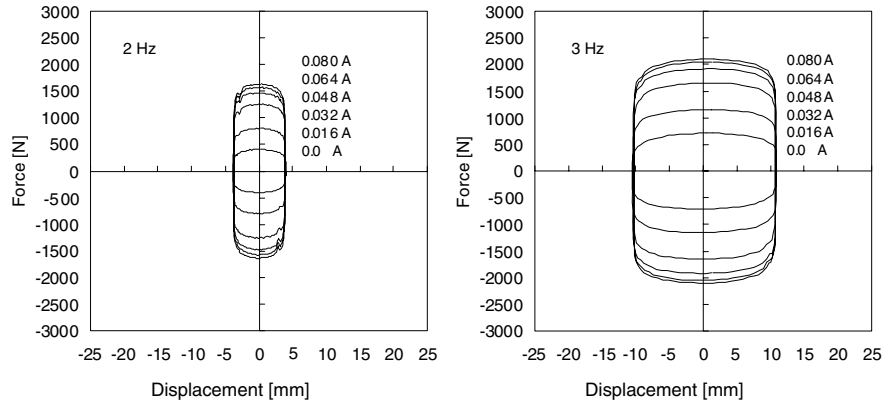


Fig. 16. Force–velocity relationship of 200 kN MR damper.



**Fig. 17.** Analytical results by involution model for 2 kN MR damper.

despite its simplicity. In this study, an additional spring and an additional mass are considered in the Bingham model in order to take into account the effects of the stiffness and inertia of the MR damper. The other analytical model is an involution model, in which the force–velocity relationship is expressed by

$$F = C_1 V^n \quad (1)$$

where  $F$  is the generating force of the MR damper,  $C_1$  is a nonlinear damping coefficient,  $V$  is the velocity of the piston, and  $n$  is an exponent. This equation has often been used to simulate viscous fluid dampers and can also be used to simulate the behavior of MR dampers because the damping force remains within the specified bound under the condition that  $n$  is close to zero.

Figure 17 shows the simulation results of the 2 kN MR damper obtained from the involution model. Both parameters,  $C_1$  and  $n$ , were assumed to be independent of the amplitude and the frequency. These parameters used in the simulations were determined to minimize the square of the errors between the experimental force and the analytical one. The values of the parameters are shown in Table 3. It was confirmed that the simulation results were close to the experimental results for each applied current.

**Table 3**  
Analytical model parameters for 2 kN MR damper

Current [A]	$C$ [N/(mm/s) <sup>n</sup> ]	$n$
0.000	85.6	0.40
0.016	292	0.26
0.032	576	0.20
0.048	704	0.19
0.064	752	0.19
0.080	812	0.18

The dynamic behavior of the 20 kN MR damper was also simulated by the same procedure as for the 2 kN MR damper. The simulation results are shown in Figure 18. For the 20 kN MR damper, the Bingham model with a spring element in series was also tried for the simulations, because the force–displacement loops obtained from the experimental tests had an inclination due to the stiffness of the MR damper. The parameters for both simulation models are shown in Table 4. Through a series of simulations, it was confirmed that the involution model is effective for predicting the dynamic behavior of the 20 kN MR damper. Moreover, the simulation results obtained from the Bingham model with the spring element also agree with the experimental results at the point where the direction of the piston movement reverses. Thus, it is shown that the Bingham model with the spring element can also simulate the effect of the MR damper's stiffness.

The parameter values of the analytical models for the 200 kN MR damper were derived by means of the least-squares method. In particular, the nonlinear

**Table 4**  
Analytical model parameters for 20 kN MR damper

Current [A]	Involution model		Bingham model		
	$C_1$ [kN/(mm/s) <sup>n</sup> ]	$n$	$C_b$ [kN/(mm/s)]	$P$ [kN]	$K$ [kN/mm]
0	0.065	0.91		0	
0.08	2.59	0.28	0.0387	5.99	31.5
0.16	3.84	0.28		9.13	

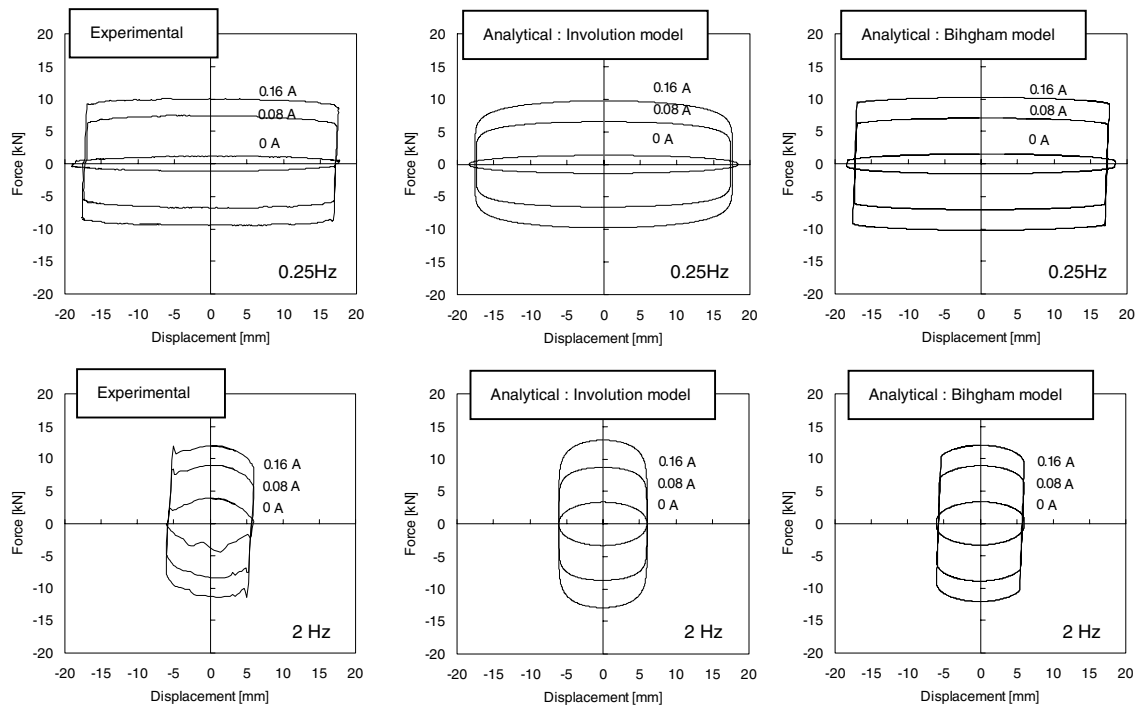


Fig. 18. Comparison between experimental and analytical results for 20 kN MR damper.

least-squares method and the Gauss-Newton method were used in the identification of the parameters for the involution model. These values are shown in Table 5. Figure 19 compares the experimental results with the analytically simulated ones under sinusoidal loading. The Bingham model with an additional mass can predict the maximum generated force and force–displacement characteristic comparatively well for each applied current. Moreover, the simulated loops under high-speed conditions, 10 cm/s and 20 cm/s, closely simulate the effect of the MR damper’s inertia. However, the simulation results of the involution model do not always agree with

the experimental ones. In particular, under high-speed conditions, 2 Hz–20 cm/s, the predicted loop is different at 0 A. It is thus necessary to set the value of  $n$  carefully, because this analytical defect by the involution model seems to be caused by the rapid change in the value of  $n$  between 0 A and 1 A.

We are going to carry out the experimental tests for random loading and random applied magnetic field in the near future. Then we would like to report those results and the comparison between the experimental results and the analytical results using our proposed models.

Table 5

Analytical model parameters for 200 kN MR damper

Current [A]	Bingham model		Involution model		
	$C_b$ [kN/(mm/s)]	$P$ [kN]	$M$ [kg]	$C_I$ [kN/(mm/s) <sup><math>q</math></sup> ]	$n$
0	0.537	0.0	4440	0.0232	1.65
1	0.487	38.9	4800	18.9	0.353
3	0.636	53.3	4480	28.0	0.330
5	0.787	63.0	3360	32.9	0.334

## 5 CONCLUSION

MR dampers with three different capacities have been developed. These dampers adopt a new mechanism, the bypass-type magnetizing orifice mechanism, and their damping characteristics have been studied experimentally and analytically. The dynamic characteristics, the force–displacement relationships and force–velocity relationships, are mainly discussed on the basis of the experimental results. The following facts were obtained through dynamic loading tests with various loading conditions. First, MR dampers that do not have a magnetic field applied to them exhibit similar dynamic behavior to typical viscous dampers. By applying the magnetic field, the generated force is increased according to the strength

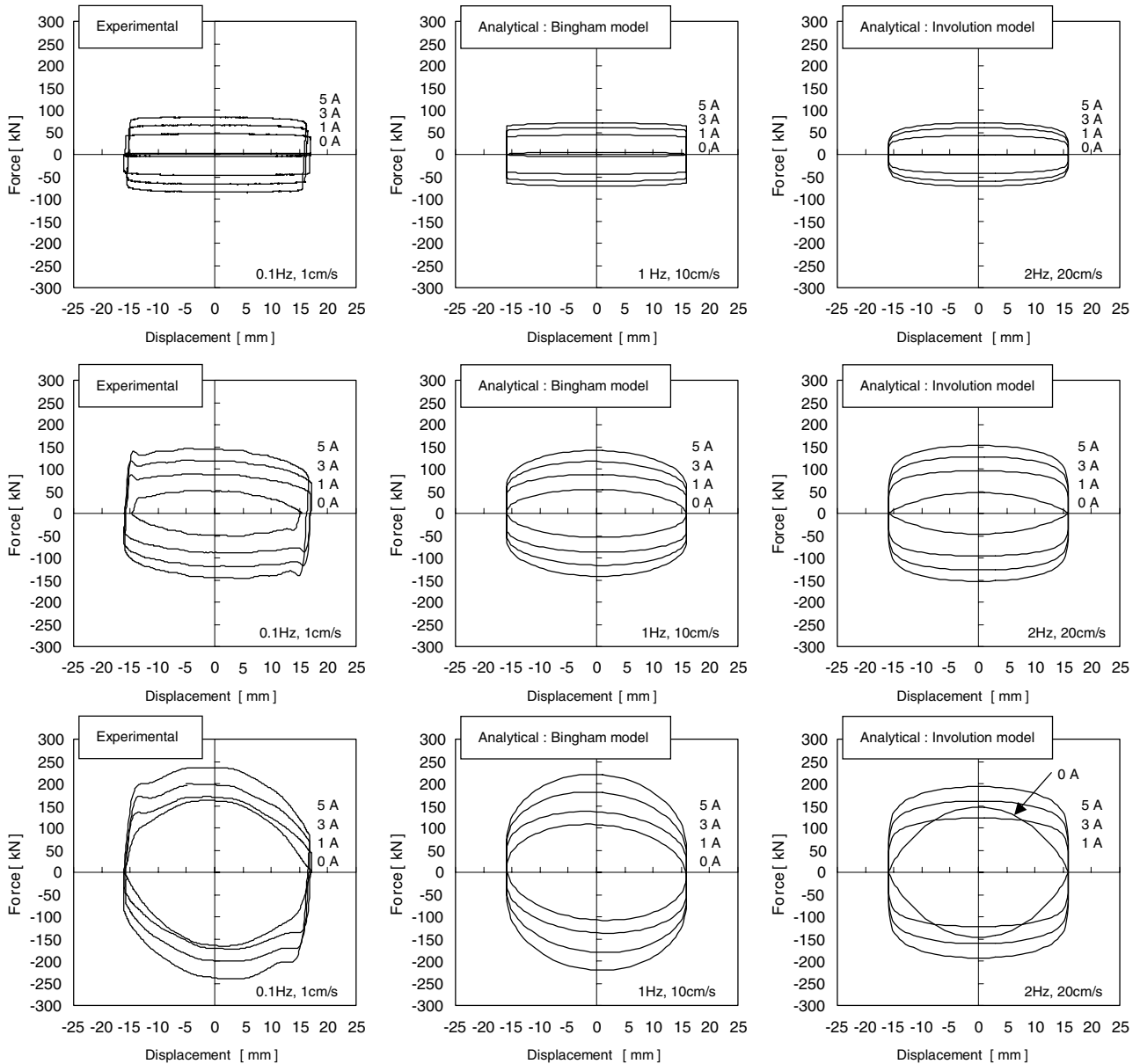


Fig. 19. Comparison between experimental and analytical results for 200 kN MR damper.

of the applied field and the behavior shifts to rigid-plastic hysteresis behavior like that of a friction damper. Second, the increase in generated force has an upper limit. Therefore, the range between the maximum force at the upper limit and the minimum force decided by the viscous force without the magnetic field is effective for variable dampers of semi-active vibration control systems. Furthermore, it was verified that the involution model and the Bingham model are suitable as a simple analytical model for the developed bypass type MR dampers.

It is clarified experimentally and analytically that the MR dampers developed in this study provide a technol-

ogy that enables semi-active control of full-scale civil engineering and building structures.

## REFERENCES

- Carlson, J. D. & Spencer, B. F. (1996), Magneto-rheological fluid dampers for semi-active seismic control, *Proceedings of the Third International Conference on Motion and Vibration Control*, **3**, 35–40.
- Johnson, E., Ramallo, J. C., Spencer, B. F. & Sain, M. K. (1998), Intelligent base isolation systems, *Proceedings of the 2nd World Conference on Structural Control*, **1**, 367–76.

- Jolly, M. R., Bender, J. W. & Carlson, J. D. (1999), Properties and applications of commercial magnetorheological fluids, *Journal of Intelligent Material Systems and Structures*, **10**, 5–13.
- Kurita, N., Kobori, T., Takahashi, M. & Niwa N. (1998), Semi-active damper system in large earthquakes, *Proceedings of the 2nd World Conference on Structural Control*, **1**, 359–66.
- Niwa, N., Kobori, T., Takahashi, M., Matsunaga, Y., Kurata, N. & Mizuno, T. (1998), Application of semi-active damper system to an actual building, *Proceedings of the 2nd World Conference on Structural Control*, **1**, 815–24.
- Spencer, B. F., Dyke, S. J., Sain, M. K. & Carlson, J. D. (1997), Phenomenological model for magnetorheological dampers, *Journal of Engineering Mechanics, ASCE*, **123**(3), 230–8.
- Spencer, B. F., Yang, G., Carlson, J. D. & Sain, M. K. (1998), “Smart” dampers for seismic protection of structures: a full-scale study, *Proceedings of the 2nd World Conference on Structural Control*, **1**, 417–26.